Optical and Quantum Electronics (2024) 56:31
https://doi.org/10.1007/s11082-023-05601-2

Design and simulation of photonic crystal fibre sensor for harmful chemicals detection in polycarbonate plastics

Abdul Mu'iz Maidi[1] · Rudi Salam[1] · Md. Abul Kalam[2] · Feroza Begum[1]

Received: 16 April 2023 / Accepted: 18 October 2023 / Published online: 23 November 2023

Abstract

A photonic crystal fiber (PCF) sensor for detecting harmful chemicals such as di(2-ethylhexyl) phthalate (DEHP), bisphenol A (BPA), and bisphenol S (BPS) in polycarbonate plastics has been proposed using fused silica as the substrate, consisting of a decagonal core hole and 2 layers of circular cladding air holes arranged in a hexagonal pattern, and numerically analysed using COMSOL Multiphysics with the Finite Element Method. The PCF sensor was evaluated for the effective area, nonlinear coefficient, chromatic dispersion, V-parameter, power fraction, relative sensitivity, and confinement loss from the visible to infrared wavelength range. The results show relative sensitivities of 99.14%, 99.93%, and 99.95% for DEHP, BPA, and BPS, respectively, at an optimum wavelength of 0.4 μm, with confinement losses ranging from 10^{-21} to 10^{-17} dB/m for all the test analytes. The design was also shown to be robust against variations in cladding air hole layers and global dimensions, making it a promising candidate for practical sensing applications in the plastic production industry. Furthermore, the sensor's ability to achieve low confinement losses, low chromatic dispersion, and a high nonlinear coefficient demonstrates its suitability for a range of other applications including optical communication, supercontinuum generation, and light illumination.

Keywords Chemical sensor · Photonic crystal fibre · Polycarbonate plastics · Relative sensitivity · Confinement loss

✉ Feroza Begum
feroza.begum@ubd.edu.bn

Abdul Mu'iz Maidi
21m5101@ubd.edu.bn

Rudi Salam
21h8458@ubd.edu.bn

Md. Abul Kalam
mdabul.kalam@uts.edu.au

[1] Faculty of Integrated Technologies, Universiti Brunei Darussalam, Jalan Tungku Link, Gadong, Bandar Seri Begawan BE1410, Brunei Darussalam

[2] School of Civil and Environmental Engineering, Faculty of Engineering and Information Technology, University of Technology Sydney, 15 Ultimo Broadway, Sydney, NSW 2007, Australia

1 Introduction

Plastic is a widely used material in daily life, commonly found in consumer products such as containers and bottles that serve essential functions. However, the presence of harmful chemicals such as di(2-ethylhexyl) phthalate (DEHP), bisphenol A (BPA), and bisphenol S (BPS) in plastics has raised significant concerns regarding their safety (Wang et al. 2022; Carli et al. 2022). Bisphenol A (BPA) is a harmful substance utilised in the production of polycarbonate plastics, epoxy resins, and some polysulfones (Rather and Wael 2013; Williams et al. 2013). Polycarbonate plastics are used in a wide range of products, including water bottles, food and water storage containers, baby bottles, utensils, medical equipment, and more (Rustagi et al. 2011). Once released, BPA acts as an endocrine-disrupting compound that can interfere with oestrogen hormones, leading to various health issues such as infertility, diabetes, obesity, behavioural changes, resistance to chemotherapy, and cancer (Rogers et al. 2013; Nomiri et al. 2019; Cimmino et al. 2020). To address these concerns, many countries have imposed regulations to limit the use of BPA, particularly in infant-related polycarbonate products. However, Bisphenol S (BPS), which is used as a substitute for BPA and is known for its heat resistance and safety, also poses similar health risks (Žalmanová et al. 2016). Additionally, di(2-ethylhexyl) phthalate (DEHP), which is utilized to add flexibility to plastics, can be found in products such as foam toys, pacifiers, mats, diapers, bed linen, and medical equipment, posing a significant risk, particularly to children who are two years old or younger (Lundin 1986; Green et al. 2005; Braun et al. 2013).

Liquid chromatography is a reliable method for detecting certain chemicals with high sensitivity and accuracy (Ballesteros-Gómez et al. 2009; Zhou et al. 2014). However, it is a laboratory technique that requires skilled professionals, specialized laboratories, and expensive equipment. Direct electrochemical analysis is another option, but it requires a high oxidation potential for detection (Dong et al. 2017). Therefore, there is a need for a sensitive, robust, and feasible detection method. Optical techniques, particularly photonic crystal fibres (PCFs), have become increasingly popular in analytical chemistry due to their unique properties. PCFs are a type of optical fibre that can be used for a variety of applications, such as nonlinear optics, medical science, and chemical and biological sensing. Hence, PCF is an ideal choice for detecting the chemicals BPA, BPS, and DEHP.

Several researchers have proposed various designs for sensing harmful chemicals in plastic components. For example, Jibon et al. (Jibon et al. 2021) highlighted the risks posed by DEHP, BPA, and BPS and proposed a PCF-based sensor to detect these chemicals. The sensor design includes a circular core hole (diameter $d = 1.4$ µm) with surrounding elliptical air holes ($d_m = 0.45$ µm and $d_n = 0.6$ µm) arranged in a "floral layer". Additionally, four layers of cladding air holes consisting of circular and elliptical holes in a dodecagonal arrangement were added. The second layer air holes follow $d = 0.75 \times \Lambda/2$, and the remaining holes are determined by $d = 0.54 \times \Lambda/2$. This complicated architecture yielded relative sensitivities of 94.9% for DEHP, 96.5% for BPA, and 97.6% for BPS at the optimum wavelength. Niger and Hasin (2019) recommended a different PCF design for the same purpose. The sensor architecture is based on Zeonex material and includes a large square core hole with square and rectangular air holes in the cladding cavity. The square core hole measures 500 µm in length for analyte infiltration, and the first layer has square holes with a length of 240 µm, while the other layers have rectangular holes of different lengths (R1 = 1020 µm, R2 = 250 µm, R3 = 850 µm and R4 = 220 µm). This PCF sensor is considered a large-scale design of a total fibre diameter of 1.25 mm and resulted in relative sensitivities over 94% for all test analytes, with 94.3% for DEHP, 95.8 for BPA, and 96.1% for BPS.

Previous intricate designs of PCFs (Jibon et al. 2021; Niger and Hasin 2019) have demonstrated reasonable relative sensitivity in the detection of chemicals such as BPA, DEHP, and BPS within plastic materials. However, these earlier designs often necessitated the use of distinct raw materials, resulting in reduced cost-effectiveness when considering large-scale applications. Moreover, it has become evident that for highly sensitive sensing purposes, a smaller microstrucuted design suffices. Considering these factors, this study introduced a novel PCF design characterised by its simplicity, cost-effectiveness, and outstanding sensing capabilities. Operating in the visible to infrared wavelength range of 0.4–2.8 µm, the proposed design features a single decagonal core hole complemented by two layers of circular cladding air holes, arranged in a hexagonal lattice. This innovative structural arrangement leads to significantly improved optical and sensing outcomes, with relative sensitivities consistently exceeding 99%, and confinement losses remaining impressively low, ranging from 10^{-21} to 10^{-17} dB/m for all the test analytes.

2 Design

The proposed PCF sensor for chemical detection, shown in Fig. 1, presents a significant improvement over prior designs due to its simple configuration. It comprises the core, cladding, and Perfectly Matched Layer (PML). The core is positioned as the centre of the fibre, and it is a decagonal hollow core that allows for the penetration of analytes, with a length denoted as l. The cladding region is designed with 18 hexagonally arranged air holes in 2 layers, each with a diameter of d, and pitch distance Λ between corresponding air holes, to reduce the refractive index for proper light confinement. Furthermore, a PML encompasses the entire structure of the fibre sensor, preventing the leakage of light.

The novel PCF sensor design has been formulated to detect the different harmful chemicals in polycarbonate plastics within the visible and infrared (IR) domain. The study encompasses an examination of the refractive indices n pertaining to the test analytes of chemicals, namely DEHP (n = 1.4870), BPA (n = 1.5850), and BPS (n = 1.6450) (Jibon et al. 2021; Niger and Hasin 2019). The envisaged operating wavelength range for this sensor spans from 0.4 to 2.8 µm.

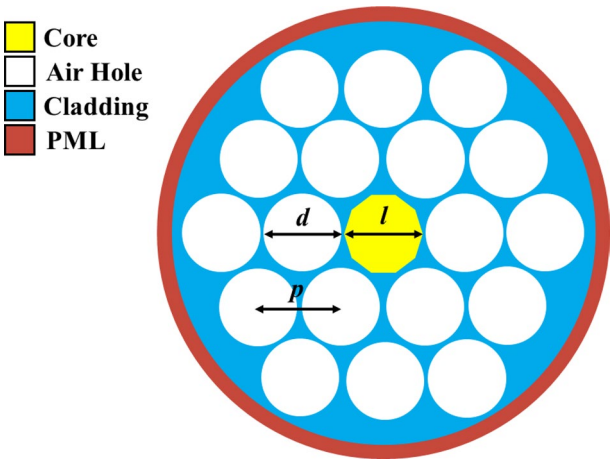

Fig. 1 Proposed PCF design for chemical detection in polycarbonate plastics

The proposed PCF, despite its hollow core, undergoes infiltration with test analytes (DEHP, BPA, and BPS). This results in the core having a refractive index higher than that of the surrounding cladding (approximately n ≈ 1.00). Consequently, the predominant light guiding mechanism employed by this PCF is the modified Total Internal Reflection (m-TIR). Within this mechanism, light is efficiently guided through the core of the PCF via a combination of total internal reflection occurring at the core-cladding boundary, and reflection facilitated by the presence of air holes within the cladding region.

To accommodate fabrication feasibility, a total diameter of 15.3 µm is achieved that follows a d/Λ ratio of 0.90, with 10% of the cladding space between air holes. The core length l is 2.7 µm, air hole diameter d is 2.7 µm with pitch distance $\Lambda = 3.0$ µm. A PML with a width of 10% of the total fibre diameter is set to absorb light leakage, which is a commonly accepted value in numerical studies (Islam et al. 2019; Ahmed et al. 2017). Fused silica is selected as the substrate with the refractive index n determined with respect to operating wavelength (Habib et al. 2021, 2022):

$$n^2 = 1 + \frac{0.69617\lambda^2}{\lambda^2 - 0.0684^2} + \frac{0.40794\lambda^2}{\lambda^2 - 0.11624^2} + \frac{0.89748\lambda^2}{\lambda^2 - 9.89616^2} \quad (1)$$

where λ is the operating wavelength.

Furthermore, the effects of increasing the cladding diameter on the proposed design have been studied. To increase the cladding diameter, more cladding air hole layers are added, resulting in a cladding structure with three and four layers. The addition of more cladding air hole layers allows for a lower refractive index of the cladding, which shall influence the optical and sensing results. Similarly, the cladding diameter has also been decreased by removing a cladding air hole layer to see its impact.

In the proposed experimental setup for the sensing mechanism, the sensor employs a comprehensive configuration that comprises essential components: precise alignment of a high-intensity light source, the proposed PCF sensor, single-mode fibres (SMFs) for optical signal transmission, an optical spectrum analyser (OSA) for spectral characterisation, and a computer for data processing. The core of the PCF is the function for the infiltration of the test analytes and serves as the point of incidence for the incident light, guided by the SMF. The interaction between the infiltrated analyte and the guided light within the core of the PCF results in evanescent field effects, inducing changes in the optical properties of the propagating light. The OSA meticulously captures these spectral alterations, allowing for precise monitoring of the light-analyte interaction effects. Subsequently, the acquired data is subjected to analysis and processing by a computer, facilitating the determination of vital properties and characteristics of the test analytes.

3 Methodology

The proposed sensor design for chemical sensing in plastics is evaluated through a numerical study using COMSOL Multiphysics v5.6 mode solver, which implements the Finite Element Method (FEM) simulation technique. FEM is a mathematical method that divides the fibre structure into small segments and calculates the electromagnetic fields of each segment. A fine meshing of the design is applied, resulting in 2721 mesh vertices, 3634 triangular segments, 666 edge elements, and 90 vertex elements.

The numerical values obtained from the simulation are used to evaluate the optical and sensing parameters of the PCF sensor, operating in 0.4–2.8 µm wavelengths; the visible to

infrared wavelengths. These parameters include the effective refractive index, effective area, nonlinear coefficient, chromatic dispersion, V-parameter, power fraction, relative sensitivity, and confinement loss. The evaluation of these parameters is crucial in determining the performance of the sensor for sensing applications, but also in other applications such as optical communication, supercontinuum generation, and illumination.

Effective area of a waveguide quantifies the maximum volume of light in the total transmitting area, and it is defined as (Yakasai et al. 2019; Begum and Abas December 2018; Kaijage et al. 2013; Abbaszadeh et al. 2022; Miyagi et al. 2010):

$$A_{\text{eff}} = \frac{\left(\int_{-\infty}^{\infty}\int_{-\infty}^{\infty}|E|^2 dxdy\right)^2}{\int_{-\infty}^{\infty}\int_{-\infty}^{\infty}|E|^4 dxdy} Re\left(n_{\text{eff}}\right) \tag{2}$$

where E is the electric field and $Re(n_{\text{eff}})$ is the real part of the effective refractive index.

Nonlinear coefficient is the measure of the ability of the fibre to generate nonlinear optical effects, and it is found by Begum and Abas December (2018), Hossain et al. (2018), Agbemabiese and Akowuah (2020):

$$\gamma = \left(\frac{2\pi}{\lambda}\right)\left(\frac{n_2}{A_{\text{eff}}}\right) \tag{3}$$

where n_2 is the nonlinear refractive index.

Chromatic dispersion is the broadening of optical pulse due to the different propagation speed of different wavelengths of light, and it is defined as (Begum and Abas December 2018; Agbemabiese and Akowuah 2020; Begum et al. 2009; Hai et al. 2008):

$$D = -\frac{\lambda}{c}\frac{d^2}{d\lambda^2} Re\left(n_{\text{eff}}\right) \tag{4}$$

where c is the speed of light in free space.

V-Parameter is a dimensionless parameter that is used to determine a number of modes of an optical fibre, and it can be measured by Habib et al. (2020), Rana et al. (2016):

$$V_{\text{eff}} = \frac{2\pi}{\lambda} R\sqrt{n_{co}^2 - n_{cl}^2} \tag{5}$$

where R is the radius of the core, and n_{co} and n_{cl} are the refractive index of core and cladding, respectively.

Power fraction is the ratio of optical power in the core to the total power of the entire fibre, and it is determined by Maidi et al. (2022a, b):

$$P = \frac{(sample)\int \text{Re}\left(E_x H_y - E_y H_x\right)dxdy}{(total)\int \text{Re}\left(E_x H_y - E_y H_x\right)dxdy} \times 100 \tag{6}$$

where E_x and E_y are the electric fields in x- and y-directions, respectively, and H_x and H_y are the magnetic fields, in x- and y-directions, respectively.

Relative sensitivity measures the sensing capabilities of the PCF by the interaction between the light signal and analytes, and it is found by Maidi et al. (2022a, b):

$$S = \frac{n_r}{\text{Re}(n_{\text{eff}})} \times P \tag{7}$$

where n_r is the refractive index of the test analyte.

Confinement loss quantifies the amount of light leakage from the core, and it is defined as (Maidi et al. 2021a, b):

$$L_c = \frac{40\pi}{\ln(10)\lambda}\mathrm{Im}\left(n_{\mathrm{eff}}\right) \times 10^6 \tag{8}$$

where $\mathrm{Im}(n_{\mathrm{eff}})$ is the imaginary part of the effective refractive index.

4 Results and discussion

The mode field distribution profile of DEHP, BPA, and BPS at the optimum wavelength $\lambda = 0.4$ µm can be observed in Fig. 2. This provides valuable insights into the spatial distribution of light in the proposed PCF sensor and the interaction between the analytes and the fibre. Based on this profile, the optical and sensing parameters of the sensor are evaluated, including effective refractive index, effective area, nonlinear coefficient, chromatic dispersion, V-parameter, power fraction, relative sensitivity, and confinement loss.

Effective refractive index results of the proposed PCF sensor in detecting DEHP, BPA, and BPS in plastics are shown in Fig. 3. The results demonstrate a nonlinear decrease in effective refractive index with respect to wavelength. Notably, BPS exhibits the highest refractive index among the analytes, followed by BPA and DEHP. This correlation reflects the individual refractive index values of each analyte, with higher refractive index resulting in higher effective refractive index due to the combination of substrate and analyte refractive indices.

Effective area quantifies the amount of light transmitted through the area of the fibre and the effective area results of the proposed PCF of DEHP, BPA, and BPS chemicals across the operating wavelength range is presented in Fig. 4. The data demonstrate an increasing trend in effective area with increasing wavelength, with BPA and BPS exhibiting a linear increase and DEHP displaying a non-linear increase. This behaviour can be attributed to the confinement of light, which starts to escape to the surrounding cladding area as the wavelength increases, resulting in an increased effective area. At the optimum wavelength $\lambda = 0.4$ µm, effective areas for DEHP, BPA, and BPS are 3.47 µm^2, 3.03 µm^2, and 2.94 µm^2, respectively.

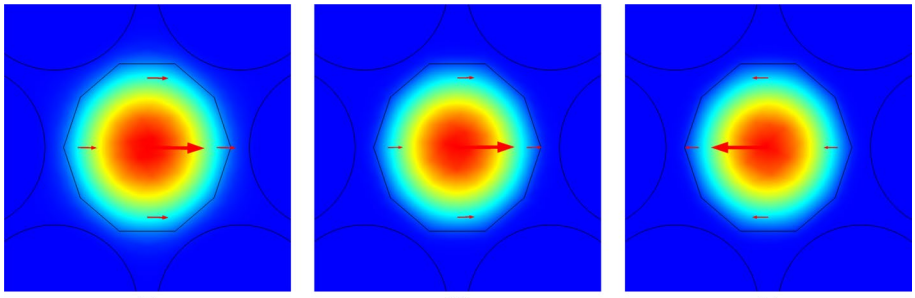

Fig. 2 Mode field profile of the proposed PCF sensor at operating wavelength of 0.4 µm for **a** DEHP **b** BPA **c** BPS

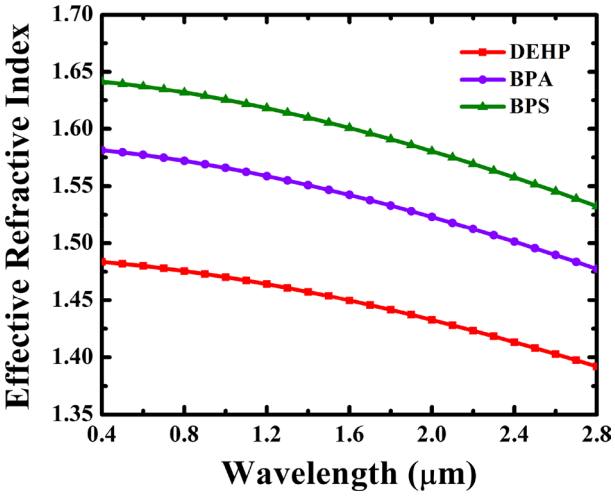

Fig. 3 Effective refractive index against operating wavelength results of the proposed PCF for DEHP, BPA, and BPS

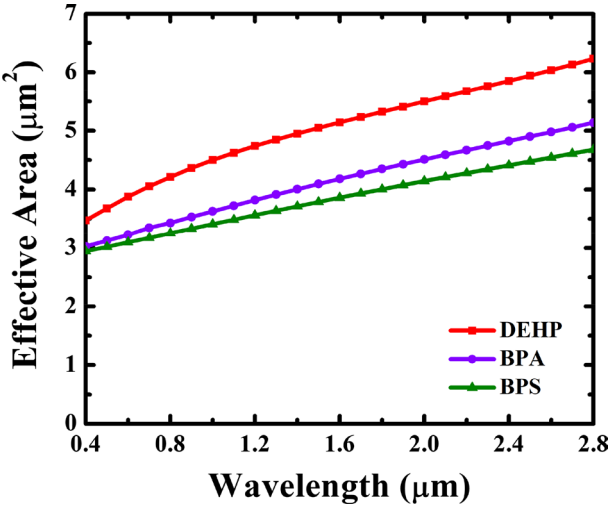

Fig. 4 Effective area against operating wavelength results of the proposed PCF for DEHP, BPA, and BPS

Equation (3) shows that nonlinear coefficient of an optical fibre is inversely proportional to its effective area. The nonlinear coefficient measures the magnitude of the nonlinear effects induced by the light beam in the waveguide of the fibre. The obtained nonlinear coefficients for all test analytes exhibit a decreasing trend with respect to wavelength, as shown in Fig. 5. This trend further suggests an inverse proportionality between nonlinear coefficient and wavelength. Specifically, DEHP demonstrates the lowest nonlinear coefficient among the analytes, followed by BPA and then BPS. The assessed nonlinear coefficients are 136 W^{-1} km^{-1} for DEHP, 156 W^{-1} km^{-1} for BPA, and 160 W^{-1} km^{-1} for BPS. These favourable high nonlinear coefficient results are advantageous for supercontinuum generation as well.

Figure 6 shows the chromatic dispersion outcomes against the wavelength of the proposed PCF sensor for DEHP, BPA, and BPS. Chromatic dispersion is defined as the quantification of the spreading of light signal as they propagate through the fibre. The

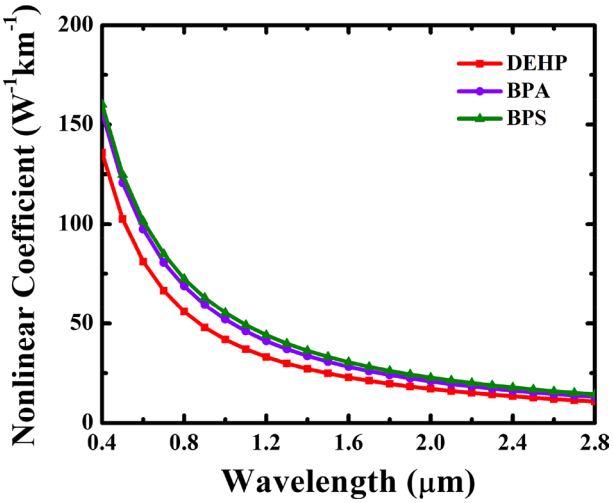

Fig. 5 Nonlinear coefficient against operating wavelength results of the proposed PCF for DEHP, BPA, and BPS

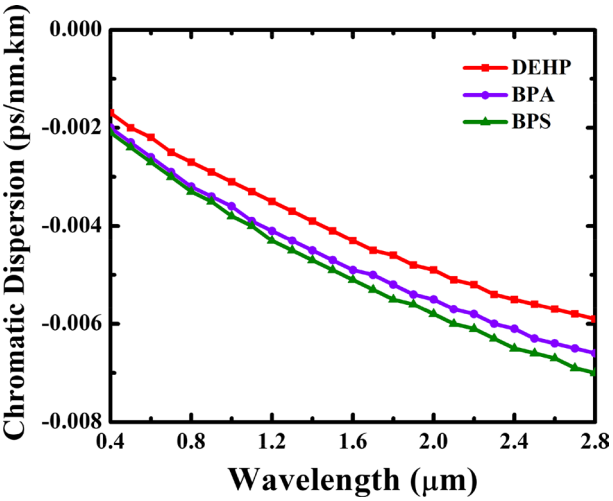

Fig. 6 Chromatic dispersion against operating wavelength results of the proposed PCF for DEHP, BPA, and BPS

results illustrate that the chromatic dispersion for the test analytes decreases with the increase in wavelength. Nevertheless, the dispersion results lie within a small range of about − 0.002 ps/nm·km to − 0.007 ps/nm·km. This indicates that the chromatic dispersion is negligible, which implies the proposed PCF design has enhanced transmission quality and reduced signal distortion. At 0.4 μm operating wavelength, the chromatic dispersions are − 0.0017 ps/nm·km, − 0.0020 ps/nm·km, and − 0.0021 ps/nm·km for DEHP, BPA, and BPS. The low dispersion values obtained at 1.55 μm also indicates its potential suitability for optical communication applications.

V-Parameter is the property for determining the number of modes in the PCF sensor. Figure 7 displays the V-Parameter results for the proposed PCF sensor in detecting DEHP, BPA, and BPS chemicals. The V-Parameter data show a decreasing curve trend across the wavelength range of 0.4–2.8 μm. According to Habib et al. (2020), Rana et al. (2016),

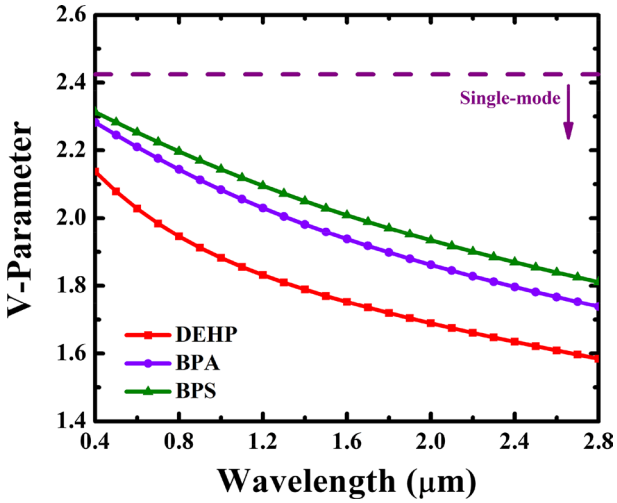

Fig. 7 V-parameter against operating wavelength results of the proposed PCF for DEHP, BPA, and BPS

V-parameter values below 2.405 indicate single-mode fibre behaviour, whereas values above 2.405 indicate multimode behaviour. Thus, the proposed PCF sensor in the study functions as a single-mode fibre for all test analytes, including DEHP, BPA, and BPS.

Power fraction is a measure of the intensity of light in the core relative to the total fibre. The power fraction results of the proposed sensor in detecting chemical analytes are presented in Fig. 8, plotted against the operating wavelength. The graph shows a decreasing trend as wavelength increases, with DEHP demonstrating an almost linear line. This observation indicates that more light is concentrated in the core at lower wavelengths. Furthermore, at the optimum wavelength of 0.4 μm, the power fraction of BPA and BPS are found to be close to each other. At the optimum operating wavelength, the power fractions for all test analytes are above 98%.

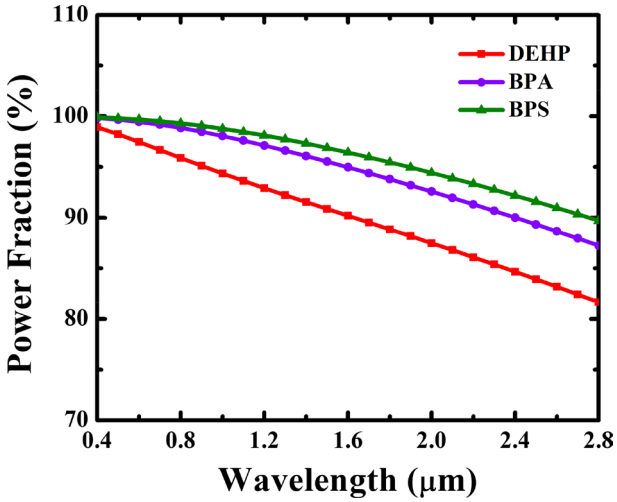

Fig. 8 Power fraction against operating wavelength results of the proposed PCF for DEHP, BPA, and BPS

Relative sensitivity is a measure of the sensing capabilities of the proposed PCF sensor, based upon the interaction between the light signal and the injected test analytes. As showcased in Fig. 9, the graph demonstrates the results of relative sensitivities of DEHP, BPA, and BPS with respect to wavelength for the proposed PCF; demonstrating almost similar trend to power fraction. Notably, there is a direct correlation between relative sensitivity and the refractive index of the analytes. BPS has the highest refractive index and yields the highest relative sensitivities, followed by BPA, and then DEHP. This conspicuous observation underscores an augmented interaction between the incident light and infiltrated analytes characterised by the relative sensitivity values. This phenomenon can be elucidated by the fundamental principles governing optical sensing within the PCF. When the refractive index of the analyte is closer to that of the background material (in this case, fused silica), the optical properties of the infiltrated medium more strongly influence the behaviour of light within the core. In essence, when the refractive index of the analyte is higher, there is a greater disparity between the refractive indices of the background material and analyte. This leads to a more pronounced changed in the optical properties of the guided light, resulting in higher sensitivity. At the optimum value, the depicted relative sensitivities are 99.14%, 99.93%, and 99.95% for DEHP, BPA, and BPS, respectively.

Figure 10 presents the confinement loss results for DEHP, BPA, and BPS chemicals in the proposed PCF sensor over the operating wavelength range. The graph illustrates that the confinement loss increases with increasing wavelength for all the test analytes. This can be attributed to the phenomenon where light signal escapes from the core and enters the cladding region as the wavelength increases. Consequently, the interaction between light and analyte decreases at higher wavelengths. The confinement of light is more effective when the refractive index of the analyte is higher than that of the substrate, as observed in this study. Specifically, BPS exhibits the lowest confinement loss, suggesting better confinement of light due to its higher refractive index than DEHP and BPA. At the wavelength of 0.4 μm, the confinement losses for DEHP, BPA, and BPS are 1.26×10^{-17} dB/m, 2.37×10^{-19} dB/m, and 8.91×10^{-21} dB/m, respectively. Furthermore, the low confinement losses observed at 1.55 μm suggest its prospective applicability in optical communication.

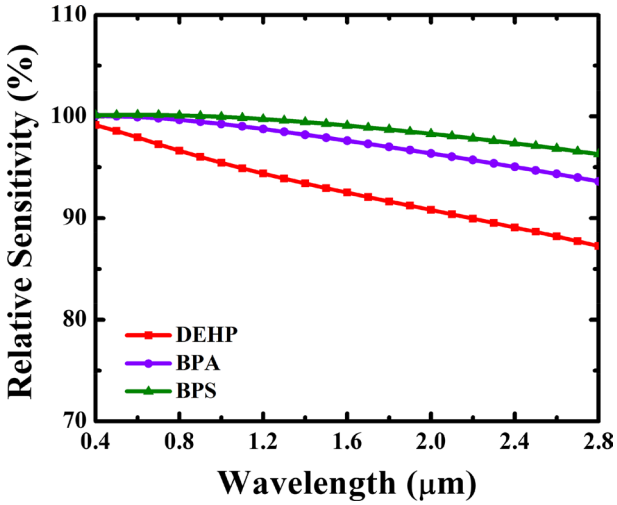

Fig. 9 Relative sensitivity against operating wavelength results of the proposed PCF for DEHP, BPA, and BPS

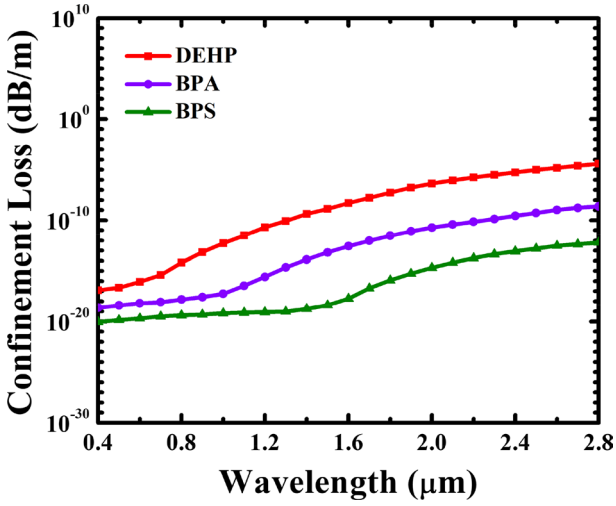

Fig. 10 Confinement loss against operating wavelength results of the proposed PCF for DEHP, BPA, and BPS

To further investigate the impact of the proposed PCF sensor design on the sensing of chemicals in plastics, variations in the cladding area were studied by adding and removing cladding air holes and layers. Figure 11 presents the effects of the varying number of cladding air hole layers by 1 and 3 rings, compared to the optimal 2 rings of cladding air hole design, on relative sensitivity. The results show overlapping data points, indicating that no significant effects were observed on the relative sensitivity of the test analytes. Therefore, the proposed PCF sensor design was found to be robust and insensitive to changes in the number of cladding air holes and layers for the detection of DEHP, BPA, and BPS chemicals.

Confinement loss variation with the number of rings of cladding air holes for the detection of the chemical test analytes against the operating wavelength is shown in Fig. 12. It is observed that as the number of cladding air hole layers is decreased, the confinement loss increases, and as the number of cladding air hole layers is increased, the confinement loss decreases. This effect is noticeable for all the test analytes: DEHP, BPA, and BPS. The reason behind this phenomenon is that by adding more air holes in the cladding region, the refractive index of the cladding reduces, resulting in a significant refractive index difference between the core and cladding. Similarly, if the cladding air hole layers are reduced, the difference in refractive index between the core and cladding becomes smaller, resulting in higher confinement losses.

Moreover, given the absence of any discernible impact on the relative sensitivity with the inclusion or exclusion of cladding air holes, further experimentation was conducted. Figure 13 shows the changes in relative sensitivity against wavelength due to 1% and 2% increments and decrements in the pitch distance and cladding air hole diameter for all test analytes (DEHP, BPA, and BPS). Results indicate that no significant effects are observed at the optimum wavelength of 0.4 μm. However, variations from the optimum results are seen as the wavelength increases. When the global dimensions are increases by 1% and 2%, relative sensitivities decrease, with 2% variations having a larger effect than 1% variations. On the other hand, when the global dimensions are decreased by 1% and 2%, relative sensitivities increase, with the results being higher for lower percentage

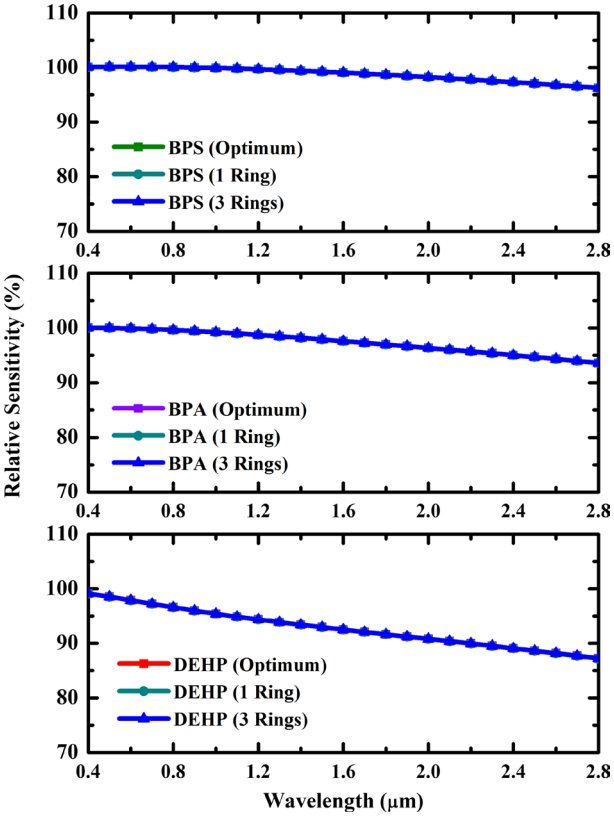

Fig. 11 Results of relative sensitivity against operating wavelength due to air hole ring variations of the proposed PCF for DEHP, BPA, and BPS

variations. Nevertheless, these variations are not substantial, indicating the robustness of the sensing capabilities and the fabrication of the proposed sensor design.

To evaluate the effects of cladding air hole rings and global dimension variations on the proposed design, relative sensitivity values at the optimum wavelength of 0.4 μm are presented in Table 1. The table compares the relative sensitivity values for the optimum design with those obtained by adding and remove cladding air hole layer and altering the global dimensions. The results suggest that even with the addition or removal of cladding air hole layers, the proposed design maintains high relative sensitivities.

Table 2 presents a comparison of the relative sensitivity results obtained using the proposed PCF sensor and prior PCFs in detecting DEHP, BPA, and BPS. The proposed PCF sensor, which features a simpler design of a single core hole and 2 layers of cladding air holes, yields higher relative sensitivities compared to complex designs. These findings suggest that a simpler PCF sensor design offers advantages, such as lower fabrication complexity, cost-effectiveness, and ease of integration in sensing methods. Therefore, the proposed PCF design is a promising candidate for practical sensing applications.

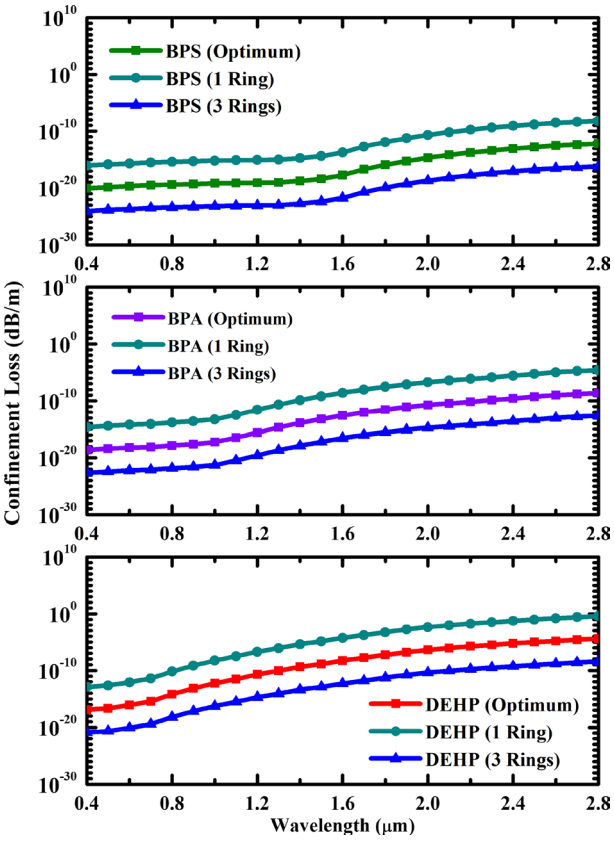

Fig. 12 Results of confinement loss against operating wavelength due to air hole ring variations of the proposed PCF for DEHP, BPA, and BPS

5 Conclusion

A simple design consisting of one decagonal core hole and two layers of circular cladding air holes arranged hexagonally has been proposed as a PCF sensor for the detection of harmful chemicals in polycarbonate plastics from visible to infrared wavelengths of 0.4–2.8 μm. The proposed structure has been modelled on COMSOL Multiphysics and numerically studied using the FEM technique, enabling visualisation of the light signal distribution in the fibre sensor. Optical and sensing parameters, such as effective refractive index, effective area, nonlinear coefficient, V-parameter, chromatic dispersion, power fraction, relative sensitivity, and confinement loss, have been assessed. Relative sensitivities yielded for DEHP, BPA, and BPS are 99.14%, 99.93%, and 99.95%, respectively, and depicted confinement losses of about 10^{-21} to 10^{-17} dB/m for all the test analytes.

Additionally, the results suggest that higher confinement of light is achieved by increasing the cladding region through the addition of more air holes, which leads to higher refractive index of the analyte than the substrate refractive index. The effects of variations in cladding air hole layers have no impact on relative sensitivity. However, minute changes in relative sensitivity were observed when global dimensions were varied. This proposed design holds promise as a practical sensing application and has the potential to improve the efficiency and accuracy of chemical analysis in plastic materials. Moreover, the remarkable

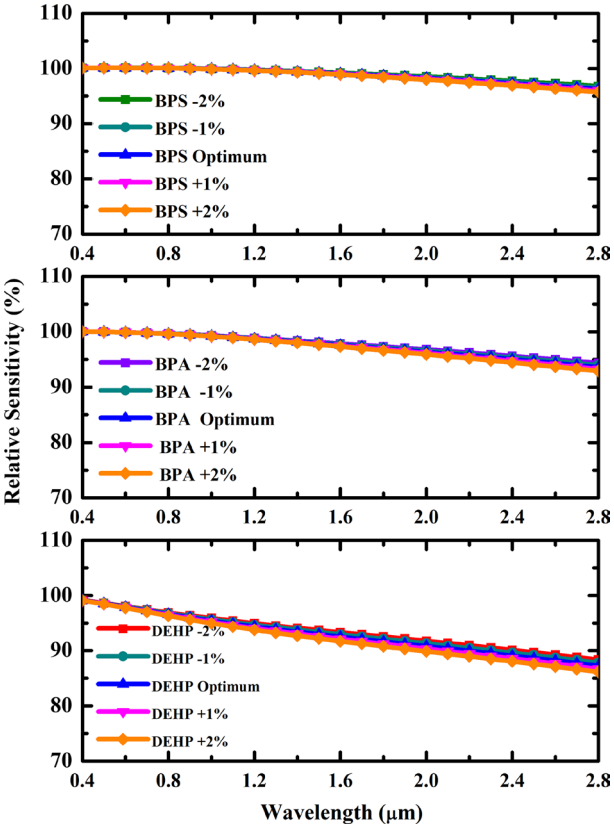

Fig. 13 Results of relative sensitivity against operating wavelength due to global dimension variations of the proposed PCF for DEHP, BPA, and BPS

Table 1 Relative sensitivity results because of variations in cladding air hole rings and global dimensions

Variation	Relative sensitivity (%)		
	DEHP	BPA	BPS
Optimum	99.14	99.93	99.95
1 cladding air hole ring	99.14	99.93	99.95
3 cladding air hole rings	99.14	99.93	99.95
+ 1% of global dimensions	99.13	99.92	99.94
− 1% of global dimensions	99.16	99.93	99.97
+ 2% of global dimensions	99.11	99.92	99.93
− 2% of global dimensions	99.18	99.94	99.98

attributes of the proposed PCF extend beyond its sensing capabilities; the obtained low confinement losses, minimal chromatic dispersion, and a notably high nonlinear coefficient position it as an enticing candidate for an array of optical applications. Notably, it can contribute to the fields of optical communication, supercontinuum generation, and visible light illumination. These versatile potential uses enhance the significance of the research and highlights the broader spectrum of applications that can benefit from this innovative PCF design. However, one primary application can be in the production stage of plastics, where

Table 2 Comparison of relative sensitivity results between the proposed PCF sensor and prior PCFs for detecting DEHP, BPA, and BPS

References	Design		Relative sensitivity (%)		
	Core	Cladding	DEHP	BPA	BPS
Jibon et al. (2021)	1 square core hole	3 layers of square and rectangular holes in a slotted arrangement	94.90	96.50	97.60
Niger and Hasin (2019)	1 circular core hole	5 layers of elliptical and circular holes in dodecagonal lattice	94.30	95.80	96.10
Proposed PCF	1 decagonal hole	2 layers of circular air holes in hexagonal lattice	99.14	99.93	99.95

the PCF sensor can ensure the health grade of plastics for human use, further enhancing its practicality and impact. On the other hand, it is essential to acknowledge the limitations inherent from this simulation-based study. To address this, the future work will encompass the fabrication of the proposed PCF sensor, followed by rigorous experimentation to validate the simulated results, thereby bridging the gap between simulation and practical applications. Moreover, the study can be extended to exploring optimisation strategies, diversifying different analyte detection, and evaluating the robustness of the proposed sensor under varying environmental conditions; these shall augment the applicability of the sensor and contribute to the continued progress of chemical sensing.

Authors' contributions Conceptualization: Abdul Mu'iz Maidi and Feroza Begum; Methodology: Abdul Mu'iz Maidi and Feroza Begum; Software: Abdul Mu'iz Maidi and Feroza Begum; Validation: Md Abul Kalam and Feroza Begum; Formal analysis: Abdul Mu'iz Maidi and Feroza Begum; Investigation: Abdul Mu'iz Maidi, Rudi Salam, and Feroza Begum; Resources: Md Abul Kalam and Feroza Begum; Data curation: Abdul Mu'iz Maidi and Feroza Begum; Writing—original draft preparation: Abdul Mu'iz Maidi; Writing—review and editing: Abdul Mu'iz Maidi and Feroza Begum; Visualization: Rudi Salam and Feroza Begum; Supervision: Feroza Begum; Project administration: Feroza Begum; Funding acquisition: Feroza Begum. All authors have read and agreed to the published version of the manuscript.

Funding This work was supported by Universiti Brunei Darussalam (UBD/RSCH/1.3/FICBF(b)/2019/008). Feroza Begum has received research support from Universiti Brunei Darussalam.

Availability of data and materials The datasets generated during and/or analysed during the current study are available from the corresponding author on reasonable request.

Declarations

Competing interests The authors declare no competing interests.

Ethical approval Not applicable.

Competing interest The authors have no relevant financial or non-financial interests to disclose.

References

Abbaszadeh, A., Makouei, S., Meshgini, S.: New hybrid photonic crystal fiber gas sensor with high sensitivity for ammonia gas detection. Can. J. Phys. **100**(2), 129–137 (2022). https://doi.org/10.1139/cjp-2021-0016

Agbemabiese, P.A., Akowuah, E.K.: Numerical analysis of photonic crystal fiber of ultra-high birefringence and high nonlinearity. Sci. Rep. **10**(1), 21182 (2020). https://doi.org/10.1038/s41598-020-77114-x

Ahmed, K., Chowdhury, S., Paul, B.K., Shadidul Islam, M., Sen, S., Ibadul Islam, M., Asaduzzaman, S.: Ultrahigh birefringence, ultralow material loss porous core single-mode fiber for Terahertz wave guidance. Appl. Opt. **56**(12), 3477 (2017). https://doi.org/10.1364/AO.56.003477

Ballesteros-Gómez, A., Rubio, S., Pérez-Bendito, D.: Analytical methods for the determination of bisphenol A in food. J. Chromatogr. A **1216**(3), 449–469 (2009). https://doi.org/10.1016/j.chroma.2008.06.037

Begum, F., Abas, P.E.: Near infrared supercontinuum generation in silica based photonic crystal fiber. Prog. Electromagn. Res. C **2019**(89), 149–159 (2018). https://doi.org/10.2528/PIERC18100102

Begum, F., Namihira, Y., Razzak, S.M.A., Kaijage, S.F., Hai, N.H., Miyagi, K., Higa, H., Zou, N.: Flattened chromatic dispersion in square photonic crystal fibers with low confinement losses. Opt. Rev. **16**(2), 54–58 (2009). https://doi.org/10.1007/s10043-009-0011-x

Braun, J.M., Sathyanarayana, S., Hauser, R.: Phthalate exposure and children's health. Curr. Opin. Pediatr. **25**(2), 247–254 (2013). https://doi.org/10.1097/MOP.0b013e32835e1eb6

Carli, F., Ciociaro, D., Gastaldelli, A.: Assessment of exposure to Di-(2-Ethylhexyl) phthalate (DEHP) metabolites and bisphenol A (BPA) and Its importance for the prevention of cardiometabolic diseases. Metabolites **12**(2), 167 (2022). https://doi.org/10.3390/metabo12020167

Cimmino, I., Fiory, F., Perruolo, G., Miele, C., Beguinot, F., Formisano, P., Oriente, F.: Potential mechanisms of bisphenol A (BPA) contributing to human disease. Int. J. Mol. Sci. **21**(16), 5761 (2020). https://doi.org/10.3390/ijms21165761

Dong, X., Qi, X., Liu, N., Yang, Y., Piao, Y.: Direct electrochemical detection of bisphenol A using a highly conductive graphite nanoparticle film electrode. Sensors **17**(4), 836 (2017). https://doi.org/10.3390/s17040836

Green, R., Hauser, R., Calafat, A.M., Weuve, J., Schettler, T., Ringer, S., Huttner, K., Hu, H.: Use of Di(2-Ethylhexyl) phthalate-containing medical products and urinary levels of mono(2-Ethylhexyl) phthalate in neonatal intensive care unit infants. Environ. Health Perspect. **113**(9), 1222–1225 (2005). https://doi.org/10.1289/ehp.7932

Habib, A., Anower, S., Haque, I.: Highly sensitive hollow core spiral fiber for chemical spectroscopic applications. Sens. Int. **1**, 100011 (2020). https://doi.org/10.1016/j.sintl.2020.100011

Habib, M.A., Anower, M.S., AlGhamdi, A., Faragallah, O.S., Eid, M.M.A., Rashed, A.N.Z.: Efficient way for detection of alcohols using hollow core photonic crystal fiber sensor. Opt. Rev. **28**(4), 383–392 (2021). https://doi.org/10.1007/s10043-021-00672-6

Habib, M.A., Abdulrazak, L.F., Magam, M., Jamal, L., Qureshi, K.K.: Design of a highly sensitive photonic crystal fiber sensor for sulfuric acid detection. Micromachines **13**(5), 670 (2022). https://doi.org/10.3390/mi13050670

Hai, N.H., Namihira, Y., Kaijage, S.F., Kinjo, T., Begum, F., Abdur Razzak, S.M., Zou, N.: A unique approach in ultra-flattened dispersion photonic crystal fibers containing elliptical air-holes. Opt. Rev. **15**(2), 91–96 (2008). https://doi.org/10.1007/s10043-008-0013-0

Hossain, M., Podder, E., Adhikary, A., Al-Mamun, A.: Optimized hexagonal photonic crystal fibre sensor for glucose sensing. Adv. Res. **13**(3), 1–7 (2018). https://doi.org/10.9734/AIR/2018/38972

Islam, M.S.M.R., Kabir, M.F., Talha, K.M.A., Islam, M.S.M.R.: A Novel hollow core terahertz refractometric sensor. Sens. Bio-Sens. Res. **25**, 100295 (2019). https://doi.org/10.1016/j.sbsr.2019.100295

Jibon, R.H., Ahmed, M., Hasan, M.K.: Identification of detrimental chemicals of plastic products using PCF in the THz regime. Meas. Sensors **17**, 100056 (2021). https://doi.org/10.1016/j.measen.2021.100056

Kaijage, S.F., Ouyang, Z., Jin, X.: Porous-core photonic crystal fiber for low loss Terahertz wave guiding. IEEE Photonics Technol. Lett. **25**(15), 1454–1457 (2013). https://doi.org/10.1109/LPT.2013.2266412

Lundin, A.P.: The safety of Di(2-Ethylhexyl) phthalate in patients receiving hemodialysis treatment. JAMA J. Am. Med. Assoc. **256**(20), 2817 (1986). https://doi.org/10.1001/jama.1986.03380200055014

Maidi, A.M., Abas, P.E., Petra, P.I., Kaijage, S., Zou, N., Begum, F.: Theoretical considerations of photonic crystal fiber with all uniform-sized air holes for liquid sensing. Photonics **8**(7), 249 (2021a). https://doi.org/10.3390/photonics8070249

Maidi, A.M., Yakasai, I., Abas, P.E., Nauman, M.M., Apong, R.A., Kaijage, S., Begum, F.: Design and simulation of photonic crystal fiber for liquid sensing. Photonics **8**(1), 16 (2021b). https://doi.org/10.3390/photonics8010016

Maidi, A.M., Kalam, M.A., Begum, F.: Photonic crystal fiber sensor for detecting sulfuric acid in different concentrations. Photonics **9**(12), 958 (2022a). https://doi.org/10.3390/photonics9120958

Maidi, A.M., Shamsuddin, N., Wong, W.-R., Kaijage, S., Begum, F.: Characteristics of ultrasensitive hexagonal-cored photonic crystal fiber for hazardous chemical sensing. Photonics **9**(1), 38 (2022b). https://doi.org/10.3390/photonics9010038

Miyagi, K., Namihira, Y., Razzak, S.M.A., Kaijage, S.F., Begum, F.: Measurements of mode field diameter and effective area of photonic crystal fibers by far-field scanning technique. Opt. Rev. **17**(4), 388–392 (2010). https://doi.org/10.1007/s10043-010-0072-x

Niger, M., Hasin, T.F.: Detection of harmful chemical compounds in plastics with highly sensitive photonic crystal fiber with higher nonlinear coefficient. In *2019 IEEE International Conference on Signal Processing, Information, Communication & Systems (SPICSCON)*; IEEE, 2019; pp 18–22. https://doi.org/10.1109/SPICSCON48833.2019.9065165.

Nomiri, S., Hoshyar, R., Ambrosino, C., Tyler, C.R., Mansouri, B.: A mini review of bisphenol A (BPA) effects on cancer-related cellular signaling pathways. Environ. Sci. Pollut. Res. **26**(9), 8459–8467 (2019). https://doi.org/10.1007/s11356-019-04228-9

Rana, S., Saiful Islam, M., Faisal, M., Roy, K.C., Islam, R., Kaijage, S.F.: Single-mode porous fiber for low-loss polarization maintaining terahertz transmission. Opt. Eng. **55**(7), 076114 (2016). https://doi.org/10.1117/1.OE.55.7.076114

Rather, J.A., De Wael, K.: Fullerene-C60 sensor for ultra-high sensitive detection of bisphenol-A and its treatment by green technology. Sens. Actuators B Chem. **176**, 110–117 (2013). https://doi.org/10.1016/j.snb.2012.08.081

Rogers, J.A., Metz, L., Yong, V.W.: Review: endocrine disrupting chemicals and immune responses: a focus on bisphenol-A and Its potential mechanisms. Mol. Immunol. **53**(4), 421–430 (2013). https://doi.org/10.1016/j.molimm.2012.09.013

Rustagi, N., Singh, R., Pradhan, S.: Public health impact of plastics: an overview. Indian J. Occup. Environ. Med. **15**(3), 100 (2011). https://doi.org/10.4103/0019-5278.93198

Wang, H., Gao, R., Liang, W., Wei, S., Zhou, Y., Zeng, F.: Assessment of BPA and BPS exposure in the general population in Guangzhou, China—estimation of daily intakes based on urinary metabolites. Environ. Pollut. **315**, 120375 (2022). https://doi.org/10.1016/j.envpol.2022.120375

Williams, S.A., Jasarevic, E., Vandas, G.M., Warzak, D.A., Geary, D.C., Ellersieck, M.R., Roberts, R.M., Rosenfeld, C.S.: Effects of developmental bisphenol A exposure on reproductive-related behaviors in california mice (Peromyscus Californicus): a monogamous animal model. PLoS ONE **8**(2), e55698 (2013). https://doi.org/10.1371/journal.pone.0055698

Yakasai, I.K., Abas, P.E., Ali, S., Begum, F.: Modelling and simulation of a porous core photonic crystal fibre for Terahertz wave propagation. Opt. Quantum Electron. (2019). https://doi.org/10.1007/s11082-019-1832-x

Žalmanová, T., Hošková, K., Nevoral, J., Prokešová, Š, Zámostná, K., Kott, T., Petr, J.: Bisphenol S instead of bisphenol A: a story of reproductive disruption by regretable substitution—a review. Czech J. Anim. Sci. **61**(10), 433–449 (2016). https://doi.org/10.17221/81/2015-CJAS

Zhou, X., Kramer, J.P., Calafat, A.M., Ye, X.: Automated on-line column-switching high performance liquid chromatography isotope dilution tandem mass spectrometry method for the quantification of Bisphenol A, Bisphenol F, Bisphenol S, and 11 other phenols in urine. J. Chromatogr. B **944**, 152–156 (2014). https://doi.org/10.1016/j.jchromb.2013.11.009